Diagnosis of Bundle Branch Block by Analyzing Body Surface Potential Maps

V Donis[1], MS Guillem[1], AM Climent[1], F Castells[1],
FJ Chorro[2], J Millet[1]

[1]Itaca, Universidad Politécnica de Valencia, Valencia, Spain
[2]Servicio de Cardiología, Hospital Clínico Universitario de Valencia, Valencia, Spain

Abstract

Bundle Branch Block (BBB) is a heart disease which is diagnosed by the analysis of the ECG morphology and the duration of the QRS complex. As Body Surface Potential Mapping provides more information than 12-lead ECG, this study aims to check whether studying mapping information BBB diagnosis can be improved.

Representative maps of Left BBB and of healthy subjects were obtained. Comparisons between these maps and the maps of individual subjects were made in order to check whether the results would provide a correct classification of the subjects. Specificity was 100% for both groups. Sensitivity was 100% for LBBB patients and 89% for healthy subjects.

The study concluded that ventricular depolarization in subjects with the same diagnosis have a similar pattern. With the quantitative analysis proposed, BBB patterns can be distinguished more easily than by visual inspection of the standard ECG, therefore improving BBB diagnosis.

1. Introduction

Bundle branch block (BBB) is a heart disease produced when one of the branches, or of the fascicles, of the His bundle cannot transmit the electrical impulses that cause ventricular contraction. Therefore, these impulses have to be transmitted by another path and, as a consequence, both ventricles do not contract simultaneously. Diagnosis of BBB is based on the morphology of the ECG signal and on the duration of the QRS complex [1,2].

Although the 12-lead electrocardiogram is the most used technique in cardiology, several studies have been performed in order to determine if the use of more leads would provide more information [3,4]. Body surface potential mapping (BSPM) mainly increases the amount of information recorded around the thorax [5-7], because the information content is limited if only the 6 precordial leads are available. In BSPM systems, 30 electrodes are commonly considered to account for most diagnostic information in the ECG [8,9].

Thanks to body surface potential maps, spatial and temporal information of the propagation of the electrical signal inside the heart is available. Hence, it is possible to observe the activation pattern of a concrete subject and this can be useful in the diagnosis of heart diseases. Previous studies of other heart diseases as Myocardial Infarction (MI) have proved that a BSPM system can help to improve the diagnosis of the disease [10-15]. For instance, Kornreich et al. proved that it was possible to classify MI patients in two groups (anterior and inferior) by analyzing Body Surface Potential Maps features [10]. In addition, it is possible to identify areas where the most significant features of a disease are patent [12,14].

In spite of the existence of previous studies about Bundle Branch Block (BBB) [16-19] which made use of BSPM systems, there has never been a real suggestion to improve its diagnosis based on body surface potential maps. These studies only described quantitatively different map patterns in potential maps, but this observation has had no clinical repercussion.

The present study aims to obtain body surface potential maps of different subjects with BBB in order to assess if the subjects with the same pathology have a similar activation pattern. In case similar activation patterns can be found, representative maps of each type of blockade will be generated and will be used for an automatic classification of patients, in terms of the similarity of their body surface potential maps with these representative maps.

2. Methods

2.1. Recording system

Our BSPM system [20,21] was used to obtain the ECG recordings. It is a commercial 64-lead recording system for biopotential measurements (Active One; Biosemi Amsterdam, The Neatherlands). The sample rate was 2048Hz and the quantization was of 1μV/bit. Electrodes were distributed nonuniformly in a vest placed upon the chest, with 16 electrodes on the back and 48 on the

anterior side, with a highest density at positions overlaying the heart (see Figure 1).

2.2. Population under study

Our database was composed of one-minute ECG BSPM recordings. Specifically, our database consisted of 18 recordings of BBB patients and 9 of healthy subjects. A cardiologist, blinded to the results of the study (FJC), diagnosed each subject by visual inspection of the 12-lead standard ECG. Diagnosis of subjects under study is listed in Table 1.

DIAGNOSIS	NUMBER OF PATIENTS
Complete Left BBB (LBBB)	13
Complete Right BBB & Anterior hemiblock (RBBB_AH)	3
LBBB & Ventricular Hypertrophy (LBBB_VH)	1
Anterior Hemiblock (AH)	1
Healthy	9

Table 1 Diagnosis of subjects under study.

2.3. Signal processing

Signals were processed by using Matlab 7.0 (The Mathworks Inc, Massachusetts). A high pass filter (cutoff frequency 0.5Hz) was applied to remove baseline fluctuation caused by breathing. Also, a low pass filter was applied (cutoff frequency 80Hz) to avoid the high frequency noise introduced by electromiogram interferences. Leads presenting a 50Hz component with a power higher than 1% of the total power of the lead were filtered with a Notch filter.

Standard 12 leads were obtained from the closest electrodes from the recorded 64 leads.

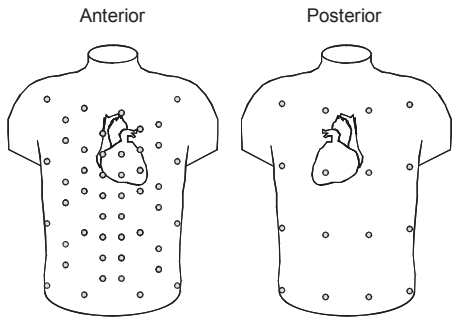

Figure 1 Electrode positioning. Left, anterior part of the thorax. Right, posterior. Each dot represents an electrode position.

Averaged cardiac cycles were obtained for each lead in every patient. First, QRS peaks were detected with a modified version of Tompkins algorithm[22], and the mean value of the RR interval was calculated. A window with a number of samples dependent on the mean RR, was taken around each complex. The window included 42% of the mean RR before the peak and 50% after the peak. After that, the median beat of each lead was calculated. Beats presenting a correlation value lower than 0.8 with the median beat were discarded in order to reject extra beats as well as noisy fragments. Non discarded beats were averaged to obtain the averaged ECG or template of each lead. All templates were visually inspected in order to discard noisy templates.

Fiducial points that correspond with the beginning (onset) and the end (offset) of the QRS interval and with the onset of the P wave and the offset of the T wave were detected by using a semi-automatic method.

Offset voltage, which is produced in the skin-electrode interface, was reduced by subtracting the mean signal value in the TP segment.

The objective was to obtain representative templates of each group of subjects with more than 5 subjects. Two groups were considered: LBBB patients and healthy subjects. In order to compute the representative templates of a group, the 64 templates of all the patients in the group should have the same length, so they were interpolated. Then, the 64 templates of all the subjects in the group were averaged. Fiducial points (onset and offset of the QRS) of each representative template were calculated.

Averaged QRS complex onset and offset were defined as it is shown in Equation 1 and Equation 2, where N is the total number of leads of the lead system. Both values were computed for each subject and for the representative templates of each group.

$$\overline{QRSonset} = \frac{1}{N}\sum_{i=1}^{N} QRSonset_i \quad (1)$$

$$\overline{QRSoffset} = \frac{1}{N}\sum_{i=1}^{N} QRSoffset_i \quad (2)$$

The averaged QRS onset and offset were considered the beginning and end of the QRS complex in order to obtain the potential maps. Fourteen body surface potential maps were computed equally spaced along the QRS complex. Maps were elaborated by using the 64 templates of each individual and the 64 averaged templates of each group, and interpolating by cubic splines the potential on the remaining surface [23].

Maps of each patient were compared with representative maps of the group he belongs to and with the representative maps of the other groups. Representative maps of the group were computed from the templates generated with the templates of every patient in the group except the patient under study.

Representative maps of the other groups were computed from the templates generated with the templates of all the patients belonging to the group.

Map comparison was performed by means of a 2D correlation. For each group and individual, the two maps computed at the beginning of the QRS complex and the two computed at the end were not considered for comparison because of their low signal level.

Correlation indexes obtained from comparisons between the ten maps of each subject and ten representative maps were averaged, providing then a single correlation value for each subject. When comparing representative maps with maps of a specific group of subjects, the mean and standard deviation of the averaged correlation indexes of the subjects in the group was computed.

A subject was considered to belong to a specific group when the averaged correlation index obtained when comparing his maps with the representative maps of the group was higher than 0.7.

3. Results

Results of the different map comparisons made are shown in Table 1. It can be observed that when the representative maps of LBBB are compared with the maps of patients suffering from this pathology the averaged correlation index is 0.85±0.05, but when they are compared with the maps of other subjects the correlation index is lower, 0.23±0.10 for healthy subjects and -0.54±0.16 for RBBB_AH subjects. Comparing LBBB representative maps with individual subjects the mean correlation index is 0.77 for the patient suffering from LBBB_HV and 0.59 for the anterior hemiblock patient.

		REPRESENTATIVE MAPS	
		LBBB	HEALTHY
COMPARISON GROUP	LBBB (N=13)	0.85±0.05	0.24±0.09
	HEALTHY (N=9)	0.23±0.10	0.82±0.10
	RBBB_AH (N=3)	-0.54±0.16	-0.24±0.10
	LBBB_VH	0.77	0.45
	AH	0.59	0.26

Table 2. Results of map comparison. N is the number of patients in each group with more than one patient. Mean correlation values of the groups composed of one subject. Average and standard deviation of the mean correlation index of the groups with more than one subject (N>1).

Regarding the comparisons of healthy representative maps, it can be observed than the higher averaged correlation index is obtained when comparing with healthy subjects, 0.82±0.10. It is lower when comparing with LBBB patients (0.24±0.09) or RBBB_AH patients (-0.24±0.10). When these representative maps are compared with the maps of a LBBB_VH patient the correlation index is 0.45 and with the maps of the anterior hemiblock patient 0.26.

Results of sensitivity and specificity tests are shown in Table 2. It can be observed that for LBBB both tests give a result of 100%, and for healthy subjects the specificity is 100% too but the sensitivity is 89%.

	LBBB	***HEALTHY***
SENSITIVITY	100%	89%
SPECIFICITY	100%	100%

Table 3. Specificity and sensitivity values for the LBBB and the HEALTHY groups.

4. Discussion and conclusions

As it has been aforementioned, mainly two features are used to diagnose BBB: QRS duration and ECG morphology. Our study focuses on QRS morphology, but as QRS onset and offset are measured QRS durations are also available. In this study, it has been proved that only when comparing the representative maps of one group of subjects with the maps of subjects belonging to the group, the correlation index is high. A 2D correlation indicates when a subject is considered to belong to a specific group. Therefore a classification of the subjects can be made, providing high values of sensitivity and specificity.

Specifically, it has been proved that when comparing the representative maps of LBBB with the patients suffering from this pathology the correlation index is high, 0.85. It is high considering that when comparing the representative maps mentioned with healthy subjects, the averaged correlation index is only 0.23, and it is -0.54 for RBBB_AH patients. As it could be expected, the correlation index is high too (0.77) when comparing these representative maps with the maps of the LBBB_VH patient, because the patient is suffering from LBBB. Finally when comparing these maps with the maps of the AH patient the correlation index is 0.59, which is not a high value neither too low, maybe it is because the beginning of the QRS can be similar in LBBB and AH because in both cases the impulse that travels through the anterior branch of the left ventricle is blocked. In fact, correlation indexes when comparing the third, fourth and fifth map of the AH subject with the representatives maps of LBBB are higher than 0.75, but they are lower for the remaining maps. In the case of the representative maps of healthy subjects, the averaged correlation index only is high when comparing with maps from healthy subjects (0.82). In other cases the correlation index is always lower than 0.5 as it could be expected.

While other BBB BSPM studies [16-19] only used BSPM information to describe the different patterns of the different types of blockade or some of their

characteristics, the results of the comparisons aforementioned could be useful to improve the diagnosis of BBB, according to its morphology, in an automated basis. As the sensitivity and specificity for LBBB patients are 100%, this can be a good method to classify the patients in the LBBB group only when they are suffering from this disease. However the sensitivity and specificity for healthy subjects is 89% and 100% respectively. Results mentioned should be contrasted by including more patients in the study.

In conclusion, in order to have more information about the propagation pattern in BBB patients BSPM systems are useful. Moreover, obtaining representative maps of a concrete type of BBB or of healthy subjects makes it possible to classify a concrete subject in the appropriate group. As a consequence, it provides an improvement in the differential diagnostic of BBB patients and maybe this technique could be also helpful for the diagnosis of other heart diseases.

Acknowledgements

This work was supported by Spanish Ministry of Education and Science under TEC2005-08401 and Universidad Politécnica de Valencia through its research iniciative program.

References

[1] Lilly Leonard S, Pathophysiology of Heart Disease. Lippincott Williams & Wilkins, 2003.

[2] Castellano C, Pérez de Juan MA, Espinosa JS, Electrocardiografía clínica. Mosby-Doyma Libros, 1996.

[3] Lux RL. Electrocardiographic body surface potential mapping. Crit Rev Biomed Eng 1982;8(3):253-79.

[4] Taccardi B, Punske BB, LUX RL, et al. Useful Lessons from Body Surface Mapping. Journal of Cardiovascular Electrophysiology 1998:9(7);773-786.

[5] Maynard S J, Menown I B A, et al. Body surface mapping improves early diagnosis of acute myocardial infarction in patients with chest pain and left bundle branch block. Heart 2003;89:998-1002.

[6] Bruns H, Eckardt L, Vahlhaus C, et al. Body surface potential mapping in patients with Brugada syndrome: right precordial ST segment variations and reverse changes in left precordial leads. Cardiovasc Res 2002:54:58-66.

[7] Hisamatsu K, Kusano KF, Morita H, et al. Usefulness of body surface mapping to differentiate patients with Brugada syndrome from patients with asymptomatic Brugada syndrome. Acta Med Okayama 2004;58(1):29-35.

[8] Kors JA, van Herpen G. How many electrodes and where? A "poldermodel" for electrocardiography. J. Electrocardiol 2002;35:7.

[9] Hoekema R, Uijen G, van Oosterom A. The number of independent signals in body surface maps. Methods Inf Med 1999;38:119.

[10] Kornreich F, Montague TJ, et al. "Qualitative and quantitative analysis of characteristic body surface potential map features in anterior and inferior myocardial infarction." Am J Cardiol 1987;60:1230-1238.

[11] Kornreich F, Montague TJ, et al. "Identification of first acute Q wave and non-Q wave myocardial infarction by multivariate analysis of body surface potential maps." Circulation 1991;84:2442-2453.

[12] Kornreich F, Montague TJ, et al. "Body surface potential mapping of ST segment changes in acute myocardial infarction." Circulation 1993;87:773-782.

[13] Medvegy M, Préda I, et al. "New body surface isopotential map evaluation method to detect minor potential losses in non-Q-wave myocardial infarction". Circulation 2000;101:1115-1121.

[14] Hänninen H, Takala P, et al. "ST-Segment level and slope in exercise-induced myocardial ischemia evaluated with body surface potential mapping." Am J Cardiol 2001;88:1152-1156.

[15] Boudik F, Anger Z, et al. "Dipyridamole body surface potential mapping: noninvasive differentiation of syndrome X from Coronary Artery Disease." J Elec 2002;35(3):181-191.

[16] Sohi GS and Flowers NC. Body Surface Map Patterns of Altered Depolarization and Repolarization in Right Bundle Branch Block. Circulation 1980;61:634-640.

[17] Sohi GS, Flowers NC et al. Comparison of Total Body Surface Map Depolarization Patterns of Left Bundle Branch Block and Normal Axis with Left Bundle Branch Block and Left-axis Deviation. Circulation 1983;67:660-664.

[18] Liebman J, Rudy Y, Diaz P, et al. The spectrum of right bundle branch block as manifested in electrocardiographic body surface potential maps. J Electrocardiol 1984;17(4):329-46.

[19] Pastore CA, Tobias N, Samesima N, et al. Body surface potential mapping investigating the ventricular activation patterns in the cardiac resynchronization of patients with left bundle-branch block and heart failure. J Electrocardiol 2006; 39(1):93-102.

[20] Guillem MS, Millet J, Bodi V, Chorro FJ.Q Wave Myocardial Infarction Analysed by Body Surface Potential Mapping. Comput Cardiol 2004;31:725.

[21] Bodí V, Sanchis J, Guillem MS, et al. Analysis of the extension of Q-waves after infarction with body surface map: relationship with infarct size. Int J Cardiol 2006; 111:399-404.

[22] Pan J, Tompkins WJ. "A real-time QRS detection algorithm." IEEE Trans Biomed Eng. 1985 Mar;32(3):230-6.

[23] Bob J. A. Schijvenaars et al. "Interpolation of Body Surface Potential Maps." J. Electrocadiology. Vol.28 Supplement, 1995; 104-109.

Address for correspondence

Victoria Donis Alagarda
ITACA. Bioingeniería. Universidad Politécnica de Valencia.
C/Camino de Vera S/N, Building 8G, 46022 Valencia, Spain
vickydonis@gmail.com